Geodesics, Parallel Transport & One-parameter Subgroups for Diffeomorphic Image Registration

Marco Lorenzi[1,2] and Xavier Pennec[1]

[1] Project Team Asclepios, INRIA Sophia Antipolis, France
[2] LENITEM, IRCCS San Giovanni di Dio, Fatebenefratelli, Brescia, Italy

Abstract. The aim of computational anatomy is to develop models for understanding the physiology of organs and tissues. The diffeomorphic non-rigid registration is a validated instrument for the detection of anatomical changes on medical images and is based on a rich mathematical background. For instance, the "large deformation diffeomorphic metric mapping" framework defines a Riemannian setting by providing an opportune right invariant metric on the tangent space, and solves the registration problem by computing geodesics parametrized by time-varying velocity fields. In alternative, stationary velocity fields have been proposed for the diffeomorphic registration based on the one-parameter subgroups from Lie groups theory. In spite of the higher computational efficiency, the geometric setting of the latter method is more vague, especially regarding the relationship between one-parameter subgroups and geodesics. In this study, we present the relevant properties of the Lie groups for the definition of geometrical properties within the one-parameter subgroups parametrization, and we define the geometric structure for computing geodesics and for parallel transporting. The theoretical results are applied to the image registration context, and discussed in light of the practical computational problems.

1 Introduction

Main objective of the computational anatomy is to develop suitable statistical models on several subjects for understanding the physiology of organs and tissues. In particular, the longitudinal observations from time series of images are an important source of information for understanding the developmental processes and the dynamics of pathologies. Thus, a reliable method for comparing different longitudinal trajectories is required, in order to develop population-based longitudinal models.

Non-rigid registration is a validated instrument for the detection of anatomical changes on medical images, and it has been widely applied on different clinical contexts for the definition of population-based anatomical atlases ([14],[9],[3]). However, in case of longitudinal data, the optimal method for comparing deformation trajectories across different subjects is still under discussion. In fact, the methods for integrating the subtle inter-subject changes into the group-wise analysis have an important impact on the accuracy and reliability of the subsequent

results. The aim is to preserve as much as possible the biological informations carried on by the different subjects, while allowing a precise comparison in a common geometric space.

Among the different techniques proposed for the comparison of longitudinal trajectories ([12],[2],[4]), *parallel transport* represents a promising method which relies on a solid mathematical background. Basically, it consists in transporting the infinitesimal deformation vector across different points by preserving its properties with respect to the space geometry, such as the parallelism.

The parallel transport has been introduced for the first time in medical imaging with the LDDMM setting [16]. LDDMM solves the image registration problem by using a Riemannian framework in which the deformations are parametrized as *diffeomorphisms* living in a suitable space, once provided an opportune right-invariant metric [10]. The registration problem is solved by computing the diffeomorphisms lying on the *geodesics* of the space parametrized by *time-varying* velocity fields under the Riemannian exponential. The setting allows the computation of the parallel transport along geodesics at the cost of a computationally intensive scheme, and this limitation prevents the application on high resolution images or large datasets.

A more efficient solution to the image diffeomorphic registration problem was introduced by the stationary velocity field (SVF) setting [1]. In this case, the diffeomorphisms are parametrized as one-parameter subgroups by *stationary* velocity fields through the Lie group exponential. This restriction allows an efficient numerical scheme for the computation but it does not directly rely on any geometric assumption on the underlying space. This implies that some important mathematical properties are not guaranteed, for instance whether the one-parameter subgroups are still geodesics or if the space is metrically complete. In spite of this lack of knowledge, the framework was found very efficient and reliable in many applications in different contexts ([8],[7],[13]) and, in [6], a framework based on the Schild's Ladder has been proposed for the evaluation of the parallel transport with the SVF.

In this paper, we investigate the relationship between Lie groups and Riemannian geometry and we highlight many interesting properties that might provide the SVF setting with part of the geometrical solidity required. In Section 2 we present the relevant properties of the Lie groups and the relationship with the Riemannian setting for the definition of the geodesics and the parallel transport. In Section 3, the results are introduced and discussed for the image registration context, while in Section 4 we show how these theoretical insights provide a clean, precise, and numerically efficient solution for the parallel transport of deformation trajectories on time series of images.

2 Lie Group and covariant differentiation

This section will recall the conceptual basis for the definition of the parallel transport along the one-parameter subgroups.

Let $\mathbb{G}$ an arbitrary finite dimensional Lie group and let $\mathfrak{g}$ the associated Lie algebra defined here with the tangent space at the identity $T_{id}\mathbb{G}$. We define the left translation L_a as the mapping $La : g \mapsto ag$, and we say that a vector field $\mathbf{X} \in T(\mathbb{G})$ is left invariant if $DL_a(\mathbf{X})_b = (\mathbf{X})_{ab}$.
There is a one-to-one correspondence between left-invariant vector fields and elements of the Lie algebra $\mathfrak{g}$, which associates to each $\mathbf{X} \in \mathfrak{g}$ the vector field defined as $\tilde{\mathbf{X}}(g) = DL_g\mathbf{X}$. The left-invariant vector fields are *complete* and their associated flow φ_t is such that $\varphi_t(g) = g\varphi_t(id)$. The association $\mathbf{X} \mapsto \varphi_1(id)$ of $\mathfrak{g}$ into $\mathbb{G}$ is called *Lie group exponential* and denoted by exp. In particular, the map exp defines the *one-parameter subgroup* associated to the vector $\mathbf{X}$ and has the following properties:

- $\varphi_t(id) = \exp(t\mathbf{X})$, for each $t \in \mathbb{R}$
- $\exp((t+s)\mathbf{X}) = \exp(t\mathbf{X})\exp(s\mathbf{X})$, for each $t, s \in \mathbb{R}$

It can be shown that the Lie group exponential is a diffeomorphism from a neighborhood of 0 in $\mathfrak{g}$ to a neighborhood of id in $\mathbf{G}$.

We are going to illustrate the transport of vectors along the exponential path $\exp(t\mathbf{X})$, and in particular the analogies with the classical Riemannian parallel transport defined for *geodesics*.

An *affine connection* on $\mathbb{G}$ is an operator which assigns to each $X \in T(\mathbb{G})$ a linear mapping $\nabla_{\mathbf{X}} : T(\mathbb{G}) \to T(\mathbb{G})$ such that

$$\nabla_{f\mathbf{X}+g\mathbf{Y}} = f\nabla_{\mathbf{X}} + g\nabla_{\mathbf{Y}} \tag{1}$$

$$\nabla_{\mathbf{X}}(f\mathbf{Y}) = f\nabla_{\mathbf{X}}(\mathbf{Y}) + (\mathbf{X}f)\mathbf{Y} \tag{2}$$

A vector field $\mathbf{X}$ is *parallel transported* along a curve $\gamma(t)$ if $\nabla_{\dot{\gamma}(t)}\mathbf{X} = 0$ for each t. In particular, a path $\gamma(t)$ on $\mathbf{G}$ is then said *geodesic* if $\nabla_{\dot{\gamma}}\dot{\gamma} = 0$. The definition generalizes the concept of "straight lines", by requiring to the tangent vector of the path to be covariantly constant.
Given a point $p \in \mathbb{G}$ and a vector $\mathbf{X} \in T_p\mathbb{G}$, there exist a unique geodesic $\gamma(t, p, \mathbf{X})$ such that at the instant $t = 0$ passes through p with velocity $\mathbf{X}$. We define therefore the *Riemannian exponential* as the application $exp : \mathbb{G}\times T(\mathbb{G}) \to \mathbb{G}$ given by $exp_p(\mathbf{X}) = \gamma(1, p, \mathbf{X})$.

If, as in the euclidean case, we want to associate to the straight lines the property of minimizing the distance between points, we need to provide the group $\mathbb{G}$ with a Riemannian manifold structure, i.e. with a metric operator g on the tangent space. In this case there is a unique symmetric connection compatible with

the metric in the sense that, for each $\mathbf{X}, \mathbf{Y}, \mathbf{Z} \in T(\mathbb{G})$ the following conditions hold:

$$\begin{aligned} \mathbf{X}\, g(\mathbf{Y}, \mathbf{Z}) &= g(\nabla_{\mathbf{X}}\mathbf{Y}, \mathbf{Z}) + g(\mathbf{X}, \nabla_{\mathbf{X}}\mathbf{Z}) && \text{(Compatibility wrt the metric)} \\ \nabla_{\mathbf{X}}\mathbf{Y} - \nabla_{\mathbf{Y}}\mathbf{X} &= [\mathbf{X}, \mathbf{Y}] && \text{(Torsion free)} \end{aligned}$$

With the choice of this special connection, called *Levi-Civita connection*, the corresponding geodesics (Riemannian geodesics) $\gamma(t)$ are the length minimizing path.

2.1 Relationship between Riemannian geodesic and one-parameter subgroups

Given a vector $\mathbf{X}$ on $T_{id}\mathbb{G}$, we can therefore define two curves on $\mathbb{G}$ passing through id and having $\mathbf{X}$ as tangent vector, one given by the Lie group exponential exp and the other given by the Riemannian exponential exp_{Id}. When do they coincide?

The connection ∇ on $\mathbb{G}$ is *left-invariant* if, for each left translation L_a ($a \in \mathbb{G}$), we have $\nabla_{DL_a\mathbf{X}}(DL_a\mathbf{Y}) = DL_a\nabla_{\mathbf{X}}(\mathbf{Y})$.

A left-invariant connection ∇ on a space $\mathbb{G}$ is a *Cartan connection* if, for any element of the Lie algebra $\mathbf{X} \in \mathfrak{g}$, the one-parameter subgroups and the Riemannian geodesics coincide, i.e. $\exp(t\mathbf{X}) = exp(t, id, \mathbf{X})$ [11].
For each left-invariant connection ∇ we can univoquely associate a product α (symmetric bilinear operator) on $T_{id}\mathbb{G}$ given by

$$\alpha(\mathbf{X}, \mathbf{Y}) = \left(\nabla_{\tilde{\mathbf{X}}}\tilde{\mathbf{Y}}\right)_{id}$$

where $\tilde{\mathbf{X}}, \tilde{\mathbf{Y}}$ are the unique left-invariant vector fields induced by the tangent vectors $\mathbf{X}, \mathbf{Y}$. We note here that a bilinear for can be uniquely decomposed as $\alpha = \alpha' + \alpha''$, where $\alpha' = \frac{1}{2}(\alpha(X,Y) + \alpha(Y,X))$ is commutative, while $\alpha'' = \frac{1}{2}(\alpha(X,Y) - \alpha(Y,X))$ is skew-symmetric.

We deduce that the condition for ∇ to be a Cartan connection is to satisfy $\alpha(\mathbf{X}, \mathbf{X}) = 0$ or, equivalently, to be skew-symmetric, for instance by assigning

$$\alpha(\mathbf{X}, \mathbf{Y}) = \lambda[\mathbf{X}, \mathbf{Y}] \tag{3}$$

In this case, the zero curvature connections are given by $\lambda = 0, 1$ (with torsion $T = -[\mathbf{X}, \mathbf{Y}]$ and $T = [\mathbf{X}, \mathbf{Y}]$ respectively) and are called *left* and *right* Cartan connections.
The choice of $\lambda = \frac{1}{2}$ lead to the *symmetric* (or *mean*) Cartan connection $\nabla_{\mathbf{X}}\mathbf{Y} = \frac{1}{2}[\mathbf{X}, \mathbf{Y}]$, with curvature $C = -\frac{1}{4}[[\mathbf{X}, \mathbf{Y}], \mathbf{Z}]$ and torsion-free. This connection is the average between left and right Cartan connection. Therefore the Cartan

connections of a Lie group are:

$$\begin{aligned}
\tilde{\nabla}_{\tilde{\mathbf{X}}}\tilde{\mathbf{Y}} &= 0 && \text{Left}\\
\tilde{\nabla}_{\tilde{\mathbf{X}}}\tilde{\mathbf{Y}} &= \frac{1}{2}\left[\tilde{\mathbf{X}},\tilde{\mathbf{Y}}\right] && \text{Symmetric}\\
\tilde{\nabla}_{\tilde{\mathbf{X}}}\tilde{\mathbf{Y}} &= \left[\tilde{\mathbf{X}},\tilde{\mathbf{Y}}\right] && \text{Right}
\end{aligned}$$

2.2 Parallel Transport on Cartan connections

Once described the conditions for the one-parameters subgroups to be geodesics, it is natural to ask how to parallel transport along these paths, and each Cartan connection lead to a specific parallel transport method.

For the left Cartan connection, the unique fields that are covariantly constant are the *left-invariant* vector fields, and the parallel transport is induced by the left multiplication, i.e. $\Pi^L : T_p\mathbb{G} \to T_q\mathbb{G}$ is defined as

$$\Pi^L(\mathbf{X}) = DL_{qp^{-1}}\mathbf{X} \tag{4}$$

Conversely, the *right-invariant* vector fields are covariantly constant with respect to to the right invariant connection. As above, the parallel transport is given by the differential of the right translation $\Pi^R(\mathbf{X}) = DR_{p^{-1}q}\mathbf{X}$. Finally, for the symmetric Cartan connection the parallel transport is given by the combination of the left and right transports. In fact it can be shown [5] that the parallel transport of $\mathbf{X}$ along the curve $\exp(t\mathbf{Y})$ is

$$\Pi^S(\mathbf{X}) = DL_{\exp(\frac{1}{2}\mathbf{Y})}DR_{\exp(\frac{1}{2}\mathbf{Y})}\mathbf{X} \tag{5}$$

3 Application to image registration

The Lie group theory is of relevant interest in the image registration context. For instance, the Lie group exponential has been already used for the diffeomorphic registration parametrized by stationary velocity fields. Of course, when moving to the infinite dimensional group of the diffeomorphisms, some caution is required for the generalization of the standard Lie theory and further research is still needed in order to quantify the impact of using such mathematical framework. However, the effectiveness of the SVF parametrization in terms of registration accuracy and computational efficiency encourage the adoption of the SVF as a valid instrument for the computational anatomy.
Given that one-parameter subgroups are geodesics for all the Cartan connections, we can implement the associated parallel transport for the SVF. Given the left and right actions on $\mathit{diff}(M)$,

$$L_f g = f \circ g \qquad R_f g = g \circ f$$

we have

$$DL_f \simeq Df \cdot g \qquad DR_f \simeq g \circ f$$

We can therefore provide an *explicit closed form formula* for the parallel transport with respect to the canonical Cartan connections. In particular, if $\mathbf{X}$ is a vector to be transported, and $\exp(t\mathbf{Y})$ is the one-parameter subgroup we have:

$$\Pi^L_{\mathbf{Y}}(\mathbf{X}) = D\exp(\mathbf{Y}) \cdot \mathbf{X} \tag{6}$$

$$\Pi^R_{\mathbf{Y}}(\mathbf{X}) = \mathbf{X} \circ \exp(\mathbf{Y}) \tag{7}$$

$$\Pi^S_{\mathbf{Y}}(\mathbf{X}) = D\exp(\frac{\mathbf{Y}}{2}) \cdot \left(\mathbf{X} \circ \exp(\frac{\mathbf{Y}}{2})\right) \tag{8}$$

Remark 1. The geodesics given by the Cartan connection are intrinsically different from the metric Riemannian ones, in the sense that the underlying connection is different from the Levi-Civita one. In particular the geodesics are not related to a positive definite from in $T\mathbb{G} \times T\mathbb{G}$. As consequence the space is not metrically complete, i.e. not all the elements of the space $\mathbb{G}$ might be reached by the one-parameter subgroups. The effect of such geometric property in the image registration context requires further investigation, in order to characterize the transformations that cannot be parametrized by SVF. However, we observe that in the image registration we are not interested in recovering "all" the possible diffeomorphisms, but only those which lead to admissible anatomical transformations.

Remark 2. From the computational point of view, we notice that among the three transport methods, Π^R requires the simple resampling of the velocity field, while both Π^L and Π^S involve the computation of the Jacobian Matrix. The involvement of high order terms can raise accuracy problems, especially in case of noisy data and numerical approximations. We can alleviate the computational inaccuracy by taking advantage of the scaling properties of the one-parameter subgroups. Rather than directly compute the Jacobian $D\exp(\mathbf{Y})$, from the property

$$\begin{aligned}\exp(\mathbf{Y}) &= \exp(\frac{\mathbf{Y}}{2}) \circ \exp(\frac{\mathbf{Y}}{2}) = \\ &= \exp(\frac{\mathbf{Y}}{n}) \circ \ldots \circ \exp(\frac{\mathbf{Y}}{n}).\end{aligned}$$

we can derive an iterative scheme for the Jacobian computation.
In fact, given a suitable first approximation $D\exp(\mathbf{Y})^{[0]} \simeq D\frac{\mathbf{Y}}{n}$ for an opportune scaling factor n, we have the iterative formula

$$D\exp(\mathbf{Y})^{[N+1]} = D\exp(\mathbf{Y})^{[N]}|_{\exp(\frac{\mathbf{Y}}{n})} \cdot D\exp(\frac{\mathbf{Y}}{n}) \tag{9}$$

Thanks to the iterative scheme (9) the Jacobian is updated for a sufficient number of small steps along the one-parameter subgroup. Thus, the scheme avoids the computation of high order quantities on the final deformation field, that could

introduce biases due to the discretization inaccuracy. In fact, the derivatives here are more robustly computed only for an opportunely scaled velocity field, and the iterative formula evaluates the final Jacobian by successive resampling and multiplications. Although the resampling scheme has an important impact on the final computational accuracy, in the following it will be performed by simple scalar interpolation.

4 Transport of longitudinal atrophy

4.1 Synthetic experiment on a simplified geometry

A synthetic progression of longitudinal atrophy was simulated on a simplified geometry, represented by a 3D gray matter sphere S_0 enclosing a white/black matter region. The atrophy was simulated by decreasing the gray layer thickness on four subsequent time points to generate the sequence S_i, $i = 1-4$ (Figure 2). The longitudinal trajectories of deformation fields $\exp(\mathbf{X}^i)$ were then evaluated by registering the images to the baseline with the Log-Demons algorithm [15]. The sequence of deformations $\exp(\mathbf{X}^i)$ was then transported on a target ellipsoidal geometry E_0 along the inter-subject deformation $\exp(\mathbf{Y})$ such that $\exp(\mathbf{Y}) * S_0 = E_0$. The transport methods that we tested were:

- Π^R,
- Π^L and Π^S with the iterative scheme,
- the conjugate action $Conj(\exp(\mathbf{X}^i)) = \exp(\mathbf{Y})\exp(\mathbf{X}^i)\exp(\mathbf{Y})^{-1}$.

Moreover, the velocity fields $\mathbf{X}^i$ were transported with the Schild's Ladder, which operates along the "diagonal" inter-subject deformations $\exp(\mathbf{Y^i})$ such that $\exp(\mathbf{Y^i}) * S_i = E_0$ (Figure 1).

The methods were quantitatively assessed by evaluating the features of interest in the ellipsoid gray layer: the average L^2 Norm of the transported stationary velocity field and the Jacobian determinant, log-Jacobian determinant and Elastic energy of the associated deformation fields. Since we are interested in preserving the interesting features of the transported trajectories, the transported quantities were compared to the original values in the reference sphere space. Moreover, the stability of the methods was tested by checking the scalar spatial maps associated to the features.

Results Table 1 shows the accuracy of the transport methods in the preservation of the measure of changes in the gray matter layer. Among the different methods, the transport Π^R was the most accurate in preserving the average measures, while the Schild's Ladder performed better on the Log-Jacobian.

From the inspection of the related scalar log-Jacobian maps (Figure 2), the transport Π^L is the less stable and leads to noisy maps. Moreover, we notice that the areas of expansions does not fit the boundary of the ellipsoid. On the

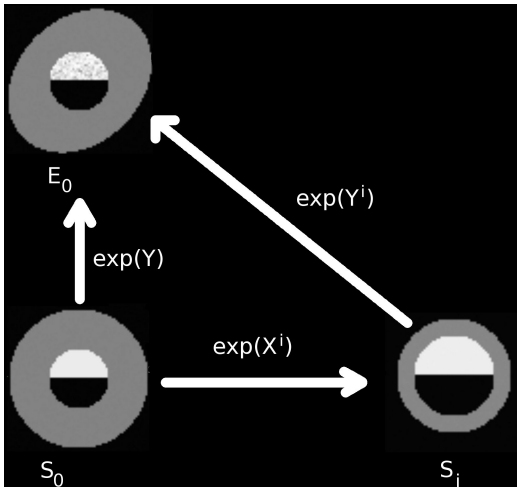

Fig. 1. Synthetic example: Intra and inter-subject variations from the sphere source space to the ellipsoid target space with related deformations.

other hand, the transport Π^R leads to smooth maps of changes, consistent with the target geometry, while the transport Π^S lies "in between", as one could reasonably expect. The Schild's Ladder lead to smooth maps as well, although the inner spherical shape seems corrupted for higher deformations. This could explain the lower performance on the quantitative measurements for the time points 3 and 4. Finally, the log-Jacobian maps associated to the conjugate actions are smooth but fail to preserve the target ellipsoidal geometry, especially for the higher deformations.

Table 1. Average measures of changes on the gray matter layer. Top-row (Source Space): changes measured on the reference sphere at each time point 1−4. Bottom-rows: changes measured from the transported longitudinal deformations on the ellipsoid. For the conjugate action it was not possible to compute the L^2 Norm of the associated stationary velocity field, since it acts on deformation fields.

	L^2 Norm				Log Jacobian				Jacobian				Elastic energy			
	1	2	3	4	1	2	3	4	1	2	3	4	1	2	3	4
Source Space	2.97	9.85	22.68	44.62	-4.77	-9.54	-14.76	-19.14	0.68	0.47	0.35	0.37	3.47	3.93	4.5	5.23
Π^L	3.02	9.57	22.14	42.32	-5	-9.82	-14.88	-20.43	**0.69**	0.51	0.43	0.45	3.51	4.01	4.67	5.53
Π^R	**2.94**	**10**	**22.81**	**44.58**	-4.70	**-9.36**	-14.51	-19.18	**0.69**	**0.49**	**0.36**	**0.37**	**3.49**	**3.9**	**4.44**	**5.15**
Π^S	3.3	11.17	25.7	50.37	-5.74	-11.2	-17.13	-23.65	**0.67**	0.50	0.42	0.48	3.58	4.2	4.99	6.05
Schild's Ladder	3.65	10.74	24.3	51.49	**-4.83**	-9.86	**-14.65**	**-19.11**	0.71	0.51	0.45	0.49	3.57	4.14	4.84	6.21
Conjugate	/	/	/	/	-2.6	-5.5	-9.18	-13.93	0.8	0.63	0.47	0.32	3.43	3.83	4.36	5.04

5 Conclusions

The study shows how the straightforward application of the Lie group theory to the diffeomorphic registration can lead to simple and efficient solutions for the transport of deformations. In particular the one-parameters subgroups are the geodesics with respect to the Cartan connections, and this mathematical setting leads to a closed form solution for the parallel transport. The geodesic of the Cartan connections generally differ from those of the Riemannian framework like the LDDMM, in the sense that they are not defined from a metric on the tangent space, and consequently the parallel transport is not related to the preservation of metric properties.
The present study highlights the trade-off between the choice of proper mathematical constructions and the related numerical implementation. In fact, among the parallel transports from the Cartan connections, the right one showed greater accuracy and smoothness, due to the simple computational requirements. However, the transport Π^R operates according to a specific geometry corresponding to the right Cartan connection. In this case, we are working in a zero-curvature space with torsion, while from the theoretical point of view it might be preferable to work with respect to a symmetric connection which leads to torsion-free spaces. At this purpose, further studies are required in order to clarify the effects in the image registration context of imposing a specific connection, and for defining more robust numerical schemes for the computation of high order quantities.

Acknowledgements This work was partially supported by the ANR program *Karametria* ANR-09-BLAN-0332 from the French Agence Nationale pour la Recherche.

References

1. V. Arsigny, O. Commowick, X. Pennec, and N. Ayache. A log-euclidean framework for statistics on diffeomorphisms. In R. Larsen, M. Nielsen, and J. Sporring, editors, *Medical Image Computing and Computer-Assisted Intervention - MICCAI*, volume 4190, page 924. Springer, Heidelberg, Sep 2006.
2. M.N. Bossa, E. Zacur, and S. Olmos. On changing coordinate systems for longitudinal tensor-based morphometry. *Spatio Temporal Image Analysis Workshop (STIA), MICCAI 2010*, 2010.
3. S. Durrleman, P. Fillard, X. Pennec, A. Trouve, and N. Ayache. Registration, atlas estimation and variability analysis of white matter fiber bundles modeled as currents. *NeuroImage*, 2011.
4. S. Durrleman, X. Pennec, A. Trouv, G. Gerig, and N. Ayache. Spatiotemporal atlas estimation for developmental delay detection in longitudinal datasets. In G. Yang, D. Hawkes, D. Rueckert, J Noble, and C. Taylor, editors, *Medical Image Computing and Computer-Assisted Intervention - MICCAI*, volume 5761. Springer, Heidelberg, Sep 2009.
5. S. Helgason. *Differential geometry, Lie groups, and symmetric spaces*. American Mathematical Soc, 1978.
6. M. Lorenzi, N. Ayache, and X. Pennec. Schilds ladder for the parallel transport of deformations in time series of images. In G. Székely and H. Hahn, editors, *Information Processing in Medical Imaging - IPMI*. Springer, Heidelberg, Jul 2011.

7. M. Lorenzi, G.B Frisoni, N. Ayache, and X. Pennec. Mapping the effects of aβ_{1-42} levels on the longitudinal changes in healthy aging: hierarchical modeling based on stationary velocity fields. In G. Fichtinger, A. Martel, and T. Peters, editors, *Medical Image Computing and Computer-Assisted Intervention - MICCAI*. Springer, Heidelberg, Sep 2011.
8. T. Mansi, X. Pennec, M. Sermesant, H. Delingette, and N. Ayache. Logdemons revisited: Consistent regularisation and incompressibility constraint for soft tissue tracking in medical images. In T. Jiang, N. Navab, J.P.W. Pluim, and M. Viergever, editors, *Medical Image Computing and Computer-Assisted Intervention - MICCAI*. Springer, Heidelberg, Sep 2010.
9. T. Mansi, I. Voigt, B. Leonardi, X. Pennec, S. Durrleman, M. Sermesant, H. Delingette, A.M. Taylor, Y. Boudjemline, G. Pongiglione, and N. Ayache. A statistical model for quantification and prediction of cardiac remodelling: Application to tetralogy of fallot. *IEEE Transactions on Medical Images*, 2011.
10. M. Miller, A. Trouvé, and L. Younes. On the metrics and Euler-Lagrange equations of computational anatomy. *Annu Rev Biomed Eng*, 4(1):375–405, 2002.
11. M.M. Postnikov. *Geometry VI*. Springer, 2001.
12. A. Rao, R. Chandrashekara, G. Sanchez-Hortiz, R. Mohiaddin, P. aljabar, J. Hajnal, B. Puri, and D. Rueckert. Spatial trasformation of motion and deformation fields using nonrigid registration. *IEEE Transactions on Medical Imaging*, 23(9), 2004.
13. C. Seiler, X. Pennec, and M. Reyes. Geometry-Aware Multiscale Image Registration Via OBBTree-Based Polyaffine Log-Demons. In G. Fichtinger, A. Martel, and T. Peters, editors, *Medical Image Computing and Computer-Assisted Intervention - MICCAI*. Springer, Heidelberg, Sep 2011.
14. P. Thompson, K.M. Ayashi, G. Zubicaray, A.L. Janke, S.E. Rose, J. Semple, D. Herman, M.S. Hong, S.S. Dittmer, D.M. Dodrell, and A.W. Toga. Dynamics of gray matter loss in alzheimer's disease. *The Journal of Neuroscience*, 23:994–1005, 2003.
15. T. Vercauteren, X. Pennec, A. Perchant, and N. Ayache. Symmetric Log-domain diffeomorphic registration: A Demons-based approach. In D. Metaxas, L. Axel, G. Fichtinger, and G. Szekely, editors, *Medical Image Computing and Computer-Assisted Intervention - MICCAI*, volume 5241, pages 754–761. Springer, Heidelberg, Sep 2008.
16. L. Younes, A. Qiu, R. Winslow, and M. Miller. Transport of relational structures in groups of diffeomorphisms. *J Math Imaging Vis*, 32(1):41–56, Sep 2008.

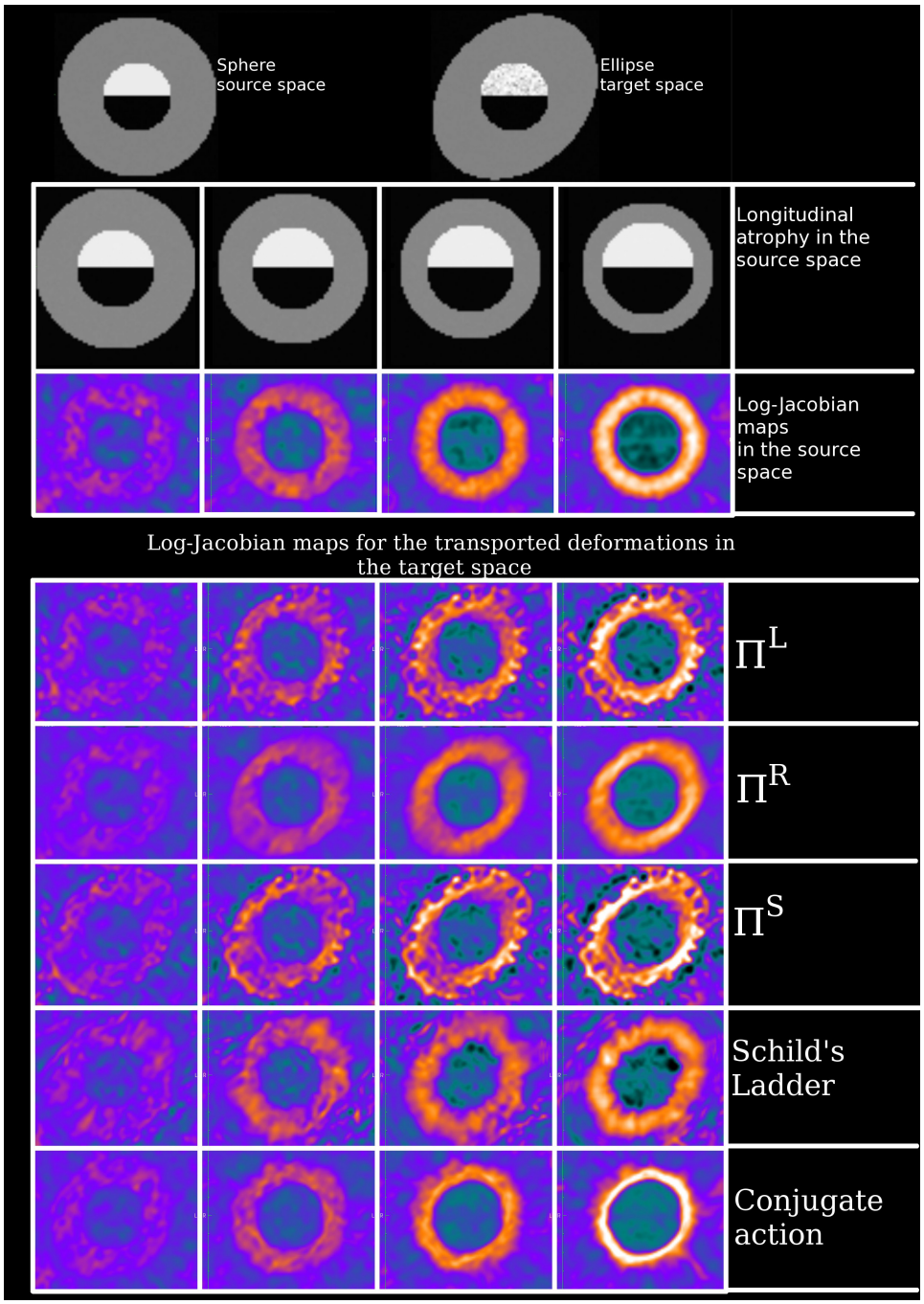

Fig. 2. Top row: Spherical source and ellipsoidal target geometrical references. From top to bottom: Longitudinal atrophy sequence in the spherical space, associated log-Jacobian determinant scalar maps, and log-Jacobian determinant maps associated to the different methods of transport.